

SHOCK WAVE STRUCTURE IN TERNARY GAS MIXTURES WITH LARGE
MOLECULAR MASS DISPARITY

G. A. Ruev, V. M. Fomin, and M. Sh. Shavaliev

UDC 533.6.011.8

No shock wave (SW) structure in a ternary gas mixture characterized by molecular mass relationship $m_1 \ll m_2 \sim m_3$ is investigated numerically by using the equations of three-velocity, three-temperature gas dynamics [1]. The velocity and temperature profiles of the mixture components are given for Mach numbers from 2 to 4 and for different values of the mixture parameters. The profiles indicate that sharp separation and large temperature differences, not only between light and heavy gases, but also among the heavy components of the mixture, occur within a SW. The temperature profiles of the heavy components in the mixture are nonmonotonic.

1. Introduction. The SW structure in gas mixtures with large molecular mass disparity cannot be described correctly within the framework of the classical Navier-Stokes equations [2]. In this case, it is necessary to use the equations of the multivelocity, multitemperature gas dynamics of gas mixtures, where each component (or group of components) of the mixture is characterized by its own macroscopic velocity and temperature. The SW structure in binary mixtures with greatly different molecular masses ($m_1/m_2 \ll 1$; m_i is the mass of a molecule of the i -th type) was investigated thoroughly in [2, 3] on the basis of these equations. In particular, it was demonstrated that drastic spatial separation of mixture components occurs within the SW, while the temperature profile of the heavy gas is nonmonotonic if its concentration is low.

We consider here the SW structure in a ternary gas mixture consisting of a light gas and two heavy gases with comparable molecular masses ($m_1 \ll m_2 \sim m_3$). This problem has not yet been investigated systematically, and there are only individual results available. The relaxation zone behind the shock front has been investigated in [4] for the limiting case of small amounts of heavy gas impurities, where the effect of heavy molecules on the light gas carrier can be neglected. The SW structure was calculated in [5] by using direct statistical simulation by means of the Monte Carlo method for the following parameters: $m_1:m_2:m_3 = 1:5:10$, $\sigma_1 = \sigma_2 = \sigma_3$ (σ_i are molecular diameters); the oncoming flow parameters were $M_0 = 5$, $n_1^0:n_2^0:n_3^0 = 100:2:1$ (M_0 is the Mach number, and n_i^0 are the densities of the number of molecules in the mixture components). Considerable separation of heavy components with respect to velocity was achieved in both cases.

The flow of ternary mixtures consisting of a light carrier gas and a binary mixture of heavy gases to be separated also occurs in devices for gas-dynamics separation of gas mixtures and isotopes (separation nozzles [6] or gas-dynamics separation elements [7]). It has been shown in [1] that a high diffusion rate and a large temperature difference can arise in such a flow between the heavy components of the mixture. They are not accounted for in the Chapman-Enskog theory, and we reached the conclusion that the equations of three-velocity, three-temperature gas dynamics must be used. It is of interest to check these results for the case of a simple flow, such as that in a two-dimensional SW.

2. Initial System of Equations and Statement of the Problem. For the unidimensional case, the system of equations of three-velocity, three-temperature gas dynamics is given by [1]

$$\begin{aligned} \partial \rho_i / \partial t + \partial \rho_i u_i / \partial x &= 0, \quad i = 1, 2, 3, \\ \rho_i \left(\frac{\partial}{\partial t} + u_i \frac{\partial}{\partial x} \right) u_i &= - \frac{\partial p_i}{\partial x} - \sum_{j=1}^3 K_{ij} u_{ij} + \frac{4}{3} \frac{\partial}{\partial x} \left(\mu_i \frac{\partial u_i}{\partial x} \right), \\ \frac{3}{2} n_i k \left(\frac{\partial}{\partial t} + u_i \frac{\partial}{\partial x} \right) T_i &= - p_i \frac{\partial u_i}{\partial x} - \sum_{j=1}^3 [q_{ij} (T_i - T_j) - \beta_{ij} K_{ij} u_{ij}^2] + \end{aligned}$$

$$\begin{aligned}
& + \frac{\partial}{\partial x} \left(\lambda_i \frac{\partial T_i}{\partial x} \right) + \frac{4}{3} \mu_i \left(\frac{\partial u_i}{\partial x} \right)^2, \\
p_i & = n_i k T_i, \quad u_{ij} = u_i - u_j, \quad \beta_{ij} = \frac{T_i}{m_i} \left(\frac{T_i}{m_i} + \frac{T_j}{m_j} \right).
\end{aligned} \tag{2.1}$$

Here, ρ_i , u_i , and T_i are the mass density, velocity, and temperature of the i -th component, $n_i = \rho_i/m_i$, and k is the Boltzmann constant. The coefficients K_{ij} and q_{ij} characterizing the exchange of momentum and energy between the mixture components and the partial coefficients of viscosity μ_i and thermal conductivity λ_i are defined by

$$\begin{aligned}
K_{1i} & = K_{i1} = \frac{16}{3} \rho_1 n_i \Omega_{1i}^{(1,1)}, \quad q_{1i} = q_{i1} = 3 \frac{k}{m_i} K_{1i}, \quad i = 2, 3, \\
K_{23} & = K_{32} = \frac{16}{3} \frac{\rho_2 \rho_3}{m_2 + m_3} \Omega_{23}^{(1,1)}, \quad q_{23} = q_{32} = \frac{3k}{m_2 + m_3} K_{23}, \\
\mu_1 & = \frac{5}{8} k T_1 \left(\Omega_1^{(2,2)} + 2 \sum_{j=2}^3 \frac{n_j}{n_1} \Omega_{1j}^{(2,2)} \right)^{-1}, \\
\lambda_1 & = \frac{75}{32} \frac{k^2 T_1}{m_1} \left(\Omega_1^{(2,2)} + 5 \sum_{j=2}^3 \frac{n_j}{n_1} \Omega_{1j}^{(1,1)} \right)^{-1}, \\
\mu_{ii} & = p_i a_{ij} a^{-1}, \quad \mu_{ij} = -p_j a_{ij} a^{-1}, \quad i, j = 2, 3, \quad j \neq i, \\
\lambda_{ii} & = \frac{5}{2} \frac{k p_i}{m_i} b_{jj} b^{-1}, \quad \lambda_{ij} = -\frac{5}{2} \frac{k p_j}{m_j} b_{ij} b^{-1}, \\
a & = \det(a_{ij}), \quad b = \det(b_{ij}), \quad i, j = 2, 3, \\
a_{ii} & = \frac{8}{5} n_i \Omega_i^{(2,2)} + \frac{32}{3} n_1 \frac{m_1}{m_i} \Omega_{1i}^{(1,1)} + \frac{16}{5} n_j M_{ji} \left(M_{ji} \Omega_{ij}^{(2,2)} + \frac{10}{3} M_{ij} \Omega_{ij}^{(1,1)} \right), \\
a_{ij} & = \frac{16}{5} n_i M_{ij} \left(M_{ji} \Omega_{ij}^{(2,2)} - \frac{10}{3} \Omega_{ij}^{(1,1)} + \frac{4}{3} M_{ij} \frac{T_i - T_j}{T_i} \Omega_{ij}^{(2,2)} \right), \\
b_{ii} & = \frac{16}{15} n_i \Omega_i^{(2,2)} + 16 n_1 \frac{m_1}{m_i} \Omega_{1i}^{(1,1)} + \frac{64}{15} n_j M_{ji}^2 \left[M_{ij} \Omega_{ij}^{(2,2)} + \frac{5}{4} M_{ji} \left(1 + 3 \frac{m_i}{m_j} \right) \Omega_{ij}^{(1,1)} \right], \\
b_{ij} & = \frac{64}{15} n_i M_{ik} M_{ji}^2 \left(\Omega_{ij}^{(2,2)} - 5 \Omega_{ij}^{(1,1)} \right), \quad M_{ij} = \frac{m_i}{m_i + m_j}.
\end{aligned} \tag{2.2}$$

In deriving (2.1) and (2.2), the lower-order terms in the expansions with respect to m_1/m_i ($i = 2, 3$) and $u_{ij}/(2kT_i/m_i + 2kT_j/m_j)^{1/2}$ were retained, while the terms that vanish in the case of the Maxwellian model of molecules were rejected. The complete expressions are given in [1].

It is necessary to find the steady-state solution of system (2.1) that satisfies the boundary conditions

$$\begin{aligned}
(\rho_i, u_i, T_i) & \rightarrow (\rho_i^0, u^0, T^0), \quad x \rightarrow -\infty, \\
(\rho_i, u_i, T_i) & \rightarrow (\rho_i^1, u^1, T^1), \quad x \rightarrow +\infty
\end{aligned} \tag{2.3}$$

(the superscript 0 denotes the oncoming flow parameters, while the quantities with the superscript 1 are related to them by the Hugoniot relationships for an equilibrium mixture).

For calculations, it is convenient to pass to dimensionless quantities,

$$\begin{aligned}
\bar{\rho}_i & = \rho_i / \rho_i^0, \quad \bar{u}_i = u_i / \sqrt{R^0 T^0}, \quad \bar{T}_i = T_i / T^0, \quad \bar{p}_i = p_i / (\rho_i^0 R^0 T^0), \\
\bar{x} & = x / L^-, \quad \bar{t} = t \sqrt{R^0 T^0} / L^-, \quad R^0 = k n^0 / \rho^0
\end{aligned}$$

(u^0 is the oncoming flow velocity). The solid sphere model was used in calculations, and the value of L^- was, therefore, borrowed from [8].

We shall limit our considerations to the case of low concentrations of heavy gases, where $n_2 \sim n_3 \ll n_1$, but $\rho_1 \sim \rho_2 \sim \rho_3$. After eliminating the terms $\sim n_i/n_1$ ($i = 2, 3$) and rendering the quantities dimensionless, Eqs. (2.1) and boundary conditions (2.3) assume the following form ($L^- = (2\pi\sigma_1^2 n^0)^{-1}$):

$$\frac{\partial \bar{\rho}_i}{\partial \bar{t}} + \frac{\partial}{\partial \bar{x}} (\bar{\rho}_i \bar{u}_i) = 0, \quad i = 1, 2, 3,$$

$$\begin{aligned}
\bar{\rho}_i \left(\frac{\partial}{\partial t} + \bar{u}_i \frac{\partial}{\partial x} \right) \bar{u}_i &= - \frac{\partial \bar{p}_i}{\partial x} - \sum_{j=1}^3 \bar{K}_{ij} \bar{u}_{ij} + \frac{4}{3} \frac{\partial}{\partial x} \left(\bar{\mu}_i \frac{\partial \bar{u}_i}{\partial x} \right), \\
\frac{3}{2} \frac{m_1}{m_i} \frac{\bar{\rho}_i}{c_1^0} \left(\frac{\partial}{\partial t} + \bar{u}_i \frac{\partial}{\partial x} \right) \bar{T}_i &= - \bar{p}_i \frac{\partial \bar{u}_i}{\partial x} - \sum_{j=1}^3 [\bar{q}_{ij} (\bar{T}_i - \bar{T}_j) - \beta_{ij} \bar{K}_{ij} \bar{u}_{ij}^2] + \\
&\quad + \frac{\partial}{\partial x} \left(\bar{\lambda}_i \frac{\partial \bar{T}_i}{\partial x} \right) + \frac{4}{3} \bar{\mu}_i \left(\frac{\partial \bar{u}_i}{\partial x} \right)^2, \quad c_1^0 = \frac{\rho_1^0}{\rho^0}, \\
\bar{\rho}_i &= 1, \quad \bar{u}_i = \bar{u}^0 = \sqrt{5/3} M_{0s}, \quad \bar{T}_i = 1, \quad \bar{x} = -l, \\
\bar{u}_i &= \bar{u}^1, \quad \bar{T}_i = \bar{T}_1, \quad \bar{x} = +l.
\end{aligned} \tag{2.4}$$

$$\tag{2.5}$$

The value of l was determined on the basis of numerical experiments in such a way that extension of the integration range did not cause changes in the results.

The dimensionless coefficients in (2.4) are determined by the following relationships:

$$\begin{aligned}
\bar{\mu}_1 &= \frac{5}{8} \sqrt{\pi c_1^0 \bar{T}_1}, \quad \bar{\mu}_i = \frac{3}{8} \sqrt{\frac{\pi}{2} \frac{c_1^0}{\bar{T}_1} \left(\frac{\sigma_1}{\sigma_{1i}} \right)^2 \frac{\bar{\rho}_i \bar{T}_i}{\bar{\rho}_1}}, \quad i = 2, 3, \\
\bar{\lambda}_1 &= \frac{15}{4c_1^0} \bar{\mu}_1, \quad \bar{\lambda}_i = \frac{5}{3c_1^0} \frac{m_1}{m_i} \bar{\mu}_i, \\
\bar{K}_{ij} &= \bar{K}_{ji} = \frac{4}{3} \frac{m_1}{m_i + m_j} (c_1^0)^{-3/2} \left(\frac{\sigma_{ij}}{\sigma_1} \right)^2 \sqrt{\frac{2m_1}{\pi} \left(\frac{\bar{T}_i}{m_i} + \frac{\bar{T}_j}{m_j} \right)} \bar{\rho}_i \bar{\rho}_j, \\
\bar{K}_{1i} &= \bar{K}_{i1} = \frac{4}{3} \frac{m_1}{m_i} (c_1^0)^{-3/2} \left(\frac{\sigma_{1i}}{\sigma_1} \right)^2 \sqrt{\frac{2}{\pi} \bar{T}_1} \bar{\rho}_1 \bar{\rho}_i, \\
\bar{q}_{1i} &= \bar{q}_{i1} = \frac{3}{c_1^0} \frac{m_1}{m_i} \bar{K}_{1i}, \quad \bar{q}_{ij} = \bar{q}_{ji} = \frac{3}{c_1^0} \frac{m_1}{m_i + m_j} \bar{K}_{ij}
\end{aligned}$$

[σ_i are the diameters of the molecules; $\sigma_{ij} = (\sigma_i + \sigma_j)/2$].

Equations (2.4) and (2.5) were solved by using the fixing method, which is based on seeking the solution of transient-state equations in a coordinate system which moves together with the wave, and subsequently arriving at the steady-state conditions. System (2.4) was approximated by using an implicit difference scheme of splitting the physical processes, which was described in detail for a binary mixture in [9].

3. Calculation Results and Discussion. The calculations were performed in the $M_0 = 2-5$ range for different concentrations, m_1/m_i , and σ_1/σ_i ($i = 2, 3$). Figures 1-7 provide the profiles of the normalized relative velocities and temperatures of the mixture components:

$$\hat{V}_i = (\bar{u}_i - \bar{u}^1)/(\bar{u}^0 - \bar{u}^1), \quad \hat{T}_i = (\bar{T}_i - 1)/(\bar{T}^1 - 1).$$

The densities of the components can hence be determined by means of the relationship $\bar{\rho}_i \bar{u}_i = \bar{u}^0$. Measurement starts at the point where the numerical density of the mixture has changed by one half of its change in the SW, i.e., $n_1^0 \hat{\rho}_1 + n_2^0 \hat{\rho}_2 + n_3^0 \hat{\rho}_3 = 0.5n^0$ for $x = 0$ ($\hat{\rho}_i = (\bar{\rho}_i - 1)/(\bar{\rho}_1^1 - 1)$, $\bar{\rho}_1^1 = \bar{u}^0/\bar{u}^1$). In Figs. 1-7, curves 1, 2, 3, 4, 5, and 6 pertain to \hat{V}_1 , \hat{V}_2 , \hat{V}_3 , \hat{T}_1 , \hat{T}_2 , and \hat{T}_3 . The parameters used in calculations are given in Table 1.

Certain characteristics of the SW structure in gas mixtures characterized by molecular mass relationship $m_1 \ll m_2 \sim m_3$ can be established by using these diagrams. At large values of M_0 (Figs. 4-6) or at very low concentrations of heavy gases (Fig. 3), there is a sharply defined shock transition zone, where the light gas parameters vary sharply, while the parameters of the heavy gases vary smoothly. This is followed by an extensive relaxation zone, where the mixture reaches the equilibrium state beyond the SW.

Nonmonotonic temperature profiles of heavy components in the mixture were obtained, as in the case of binary mixtures [2, 3]. There is a region within the SW where \hat{T}_3 and \hat{T}_2 or only \hat{T}_3 exceeds the equilibrium temperature beyond the SW (temperature peak). Depending on m_3/m_2 and σ_3/σ_2 , a large temperature peak may occur for any of the heavy gases [for instance, for the heaviest gas if $\sigma_3/\sigma_2 = 1$ (Fig. 5), and for the lighter gas if $\sigma_3/\sigma_2 = 2$ (Fig. 6)]. More intensive deceleration of the heaviest gas occurs in the latter case while more inten-

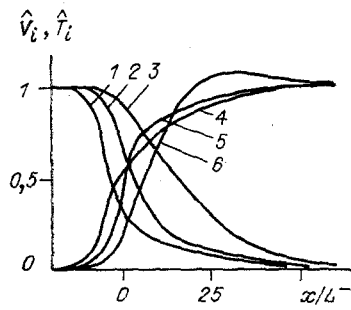


Fig. 1

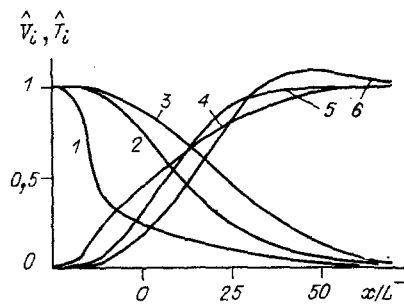


Fig. 2

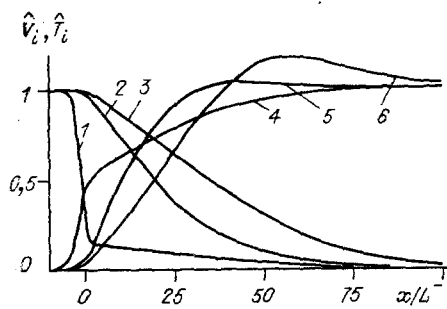


Fig. 3

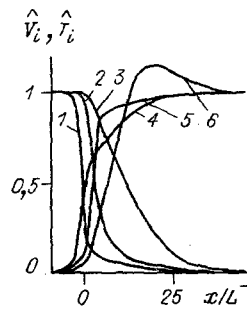


Fig. 4

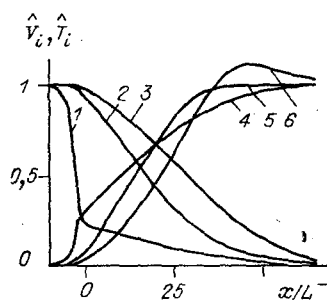


Fig. 5

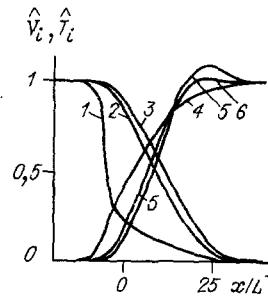


Fig. 6

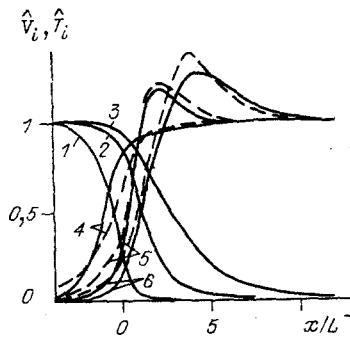


Fig. 7

TABLE 1

Fig. No.	M_0	$\frac{n_1^0}{n_2^0}$	$\frac{n_2^0}{n_3^0}$	$\frac{m_2}{m_1}$	$\frac{m_3}{m_2}$	$\frac{\sigma_2}{\sigma_1}$	$\frac{\sigma_3}{\sigma_2}$
1	2	100	1	20	4	2	1
2	3	100	1	100	2	2	1
3	3	300	1	100	2	2	1
4	4	100	1	20	4	2	1
5	4	100	1	100	2	2	1
6	4	100	1	100	2	2	2
7	5	50	2	5	2	1	1

sive deceleration of the lighter gas occurs in the first case. The temperature peak rises both with an increase in the Mach number (Figs. 1 and 4) and a reduction in the concentration of heavy gases (Figs. 2 and 3). The mechanism of the temperature peak formation in a binary mixture has been explained in [2]. A similar mechanism is operative also in a ternary mixture.

For sufficiently large values of M_0 , the temperature peak develops in both heavy components of the mixture (Fig. 7). Figure 7 also shows the results [5] (dashed curves) obtained by direct statistical simulation. In spite of the fact that the results were compared outside the scope of applicability of the initial equations [insufficient smallness of the molecular mass ratio m_i/m_1 ($i = 2, 3$) and a rather large value of the Mach number ($M_0 = 5$)], there is good qualitative agreement for the temperatures of the mixture components.

Within a SW, the mixture components are characterized by substantially different velocities and temperatures, which supports our view that the equations of three-velocity, three-temperature gas dynamics must be used. The sharp separation with respect to velocity and temperature between the light and the heavy components of the ternary mixture under consideration can be explained, as in the case of the binary mixture, by the large difference between the molecular masses. The separation between the heavy components of the mixture is caused basically by their interaction with the light gas carrier.

The development of large velocity and temperature differences and of the temperature peak in the SW for a mixture of complex molecules may intensify various activation processes. It has been demonstrated in [10] that, in chemically reacting mixtures, the creation of a large temperature difference between light and heavy molecules leads to a considerable difference between the direct reaction rate, where one of the reagents consists of light molecules, and the inverse reaction rate, as well as a considerable increase in the yield of reaction products. Considering the results given in the present paper, we can expect that similar phenomena within the SW will also arise during chemical reactions between heavy molecules of a mixture.

LITERATURE CITED

1. M. Sh. Shavaliev, Equations of Multiliquid Hydrodynamics for Gas Mixtures, ITPM Preprint, No. 28-88, Siberian Branch, Russian Academy of Sciences [in Russian], Novosibirsk (1988).
2. G. A. Ruev, V. M. Fomin, and M. Sh. Shavaliev, "Shock wave structure in gas mixtures with large mass disparity," Prikl. Mekh. Tekh. Fiz., No. 4 (1989).
3. R. Fernandez-Feria and J. F. de la Mora, "Shock wave structure in gas mixtures with large mass disparity," J. Fluid Mech., 179 (1987).
4. Ya. B. Zel'dovich, A. P. Genich, and G. B. Manelis, "Characteristics of progressive relaxation within the shock wave front in gas mixtures," Dokl. Akad. Nauk SSSR, 248, No. 2 (1979).
5. A. P. Genich, S. V. Kulikov, G. B. Manelis, et al., "Utilization of weighting schemes of statistical simulation of multicomponent gas flow in calculating the shock wave structure," ZhVMMF, 26, No. 12 (1986).
6. W. Ehrfeld and W. Schelb, "Influence of nonequilibrium effects on isotope separation in real flow fields of separation nozzles," in: V. Boffi and C. Cercignani, Rarefied Gas Dynamics, Vol. 1, Teubner, Stuttgart (1986).

7. A. V. Bulgakov, Gas-Dynamics Separation of Gas Mixtures and Isotopes in Interacting Flows, Author's abstract of dissertation for the degree of candidate of physicomathematical sciences, IT, Siberian Branch, Russian Academy of Sciences, Novosibirsk (1987).
8. G. A. Bird, Molecular Gas Dynamics, Oxford Univ. Press, New York (1976).
9. G. A. Ruev, V. M. Fomin, and M. Sh. Shavaliev, "Shock wave structure in a two-velocity, two-temperature mixture of viscous, heat-conducting gases," ChMMSS, 17, No. 2 (1986).
10. V. V. Struminskii and V. Yu. Velikodnyi, "The substantial increase in the chemical reaction rate in nonequilibrium gas mixtures," Dokl. Akad. Nauk SSSR, 295, No. 5 (1987).

ESTIMATE OF THE TEMPERATURE FIELD IN A COMPRESSIBLE
MEDIUM

T. A. Butina

UDC 539.4.012.1.536

Short-duration dynamic loading causes the development and propagation of shock waves (SW) in a continuous medium. The intensity of the shock waves depends on the intensity of the load applied and the physicomathematical characteristics of the material. As a result of high compression, the material is heated [1]. As the SW progresses, the region of material compression shifts, and the temperature of the medium changes. Estimates of the temperature field in a compressible medium and the residual heating of the material are of great interest for practical applications.

The methods for calculating the elastic potential and the temperature at the wave front are presented in [2, 3]. The Hugoniot adiabats, the atomic interaction potentials, and the Grüneisen coefficients have been determined in [4] for a number of metals. A detailed survey of the literature is provided in [5] along with an analysis of the known equations of state (see also [2, 4]). The methods of estimating the temperature on the Hugoniot adiabat and the residual temperature are given in [6-9].

The state of the continuous medium is described by the following system of equations [10]. The equation of motion is

$$\frac{\rho_0}{V} \frac{\partial u}{\partial t} = - \frac{\partial}{\partial r} (p - S_r) + \frac{(k-1)(S_r - S_\theta)}{r}, \quad (1)$$

where $V = \rho_0 / \rho$; ρ_0 and ρ are the initial and the present values of the density, respectively, u is the mass velocity, r is the present radius, p is the mean stress, and S_r and S_θ are the components of the stress deviator; $k = 1, 2,$ and 3 for the two-dimensional, cylindrical, and spherical cases, respectively.

The continuity equation is given by

$$\frac{\dot{V}}{V} = \frac{1}{r} \frac{\partial (r^{k-1} u)}{\partial r}. \quad (2)$$

with an allowance for the thermal conductivity, the energy equation is given by

$$\dot{E} = p \dot{V} - V (S_r \dot{\epsilon}_r + (k-1) S_\theta \dot{\epsilon}_\theta) + \frac{k}{r^{k-1}} \frac{\partial}{\partial r} \left(r^{k-1} \kappa \frac{\partial T}{\partial r} \right). \quad (3)$$

Here, κ is the thermal conductivity coefficient, T is the temperature, and E is the total energy. The expressions for the strain are the following:

$$\epsilon_r = \frac{\partial e}{\partial r} - \frac{1}{2} \left(\frac{\partial e}{\partial r} \right)^2, \quad \epsilon_\theta = \frac{e}{r} - \frac{1}{2} \left(\frac{e}{r} \right)^2 \quad (4)$$

Kaliningrad. Translated from *Prikladnaya Mekhanika i Tekhnicheskaya Fizika*, No. 1, pp. 23-26, January-February, 1992. Original article submitted May 10, 1990; revision submitted September 11, 1990.